

Use of Lamb Waves to Monitor Plates: Experiments and Simulations

D. W. Greve^a, J. J. Neumann^a, J. H. Nieuwenhuis^b, I. J. Oppenheim^{c*}, N. L. Tyson^c

^aDept. of Electrical and Computer Engineering, Carnegie Mellon University, Pittsburgh, PA 15213

^bFaculty of Electrical Engineering, Technical University of Vienna, Vienna, Austria

^cDept. of Civil and Environmental Engineering, Carnegie Mellon University, Pittsburgh, PA 15213

ABSTRACT

Lamb waves at ultrasonic frequencies travel with little attenuation in thin elastic plates, and we demonstrate their use in pulse-echo behavior to monitor plate integrity. We envision using a single PZT wafer-type transducer to generate waves and to receive reflections from distant flaw or boundary locations. However, Lamb waves generally have multiple modes, each of them highly dispersive, and in consequence pulse dispersion can become pronounced and can make difficult or impossible the interpretation of pulse-echo responses. We show that selective generation of the S0 wave will overcome those difficulties; therefore, selection of transducer dimensions and pulse characteristics to achieve selective generation should be considered mandatory for most intended applications. We first review the work of others identifying a basic relationship between transducer dimension and excitation frequency for selective generation of the S0 wave. We then summarize our extensive experimental studies of wafer-type transducers with particular attention to S0 and A0 mode behavior, both in transmission and reception. We next report our two-dimensional finite element simulation of the same problem performed in FEMLAB, requiring transient simulation of the coupled electromechanical problem. We simulate the piezoelectric response of the wafer-type transducer coupled to the elastic plate, both as transmitter and receiver, as well as the development of Lamb waves within the source region and their subsequent propagation along the plate. Simulations illustrate the development and separation of the S0 and A0 modes and reproduce the expected group velocities and dispersion behavior. We show good agreement between our experiments and our simulations regarding S0 mode behavior, and we summarize the results to guide a designer in choosing transducer dimensions. In particular, good selectivity between the S0 and A0 mode generation can be obtained with appropriate choice of transducer size and center frequency. We show the results of experiments on an aluminum plate in which excitation of a single PZT wafer-type transducer at 6.5 V (peak-to-peak) produces reflected signals of ample strength (tens of mV) from distant boundaries and from partial thickness flaws.

Keywords: Lamb waves, plates, piezoelectric, ultrasonics, wafer-type transducer.

1. INTRODUCTION

Guided waves in plates, also termed Lamb waves, can be used for non-destructive testing of aluminum aircraft panels and other platelike objects. Complications encountered in applying Lamb waves include the existence of multiple modes and the dispersive character of the modes [1, 2]. Figure 1 is the calculated dispersion curve showing the group velocity for harmonic S0 and A0 waves in an elastic solid material characterized by a longitudinal wave velocity of 5.88 mm/ μ s and a transverse wave velocity of 3.39 mm/ μ s. The velocity of the Lamb wave mode is a function of $f \cdot d$, the product of frequency f and plate thickness d , expressed in MHz-mm. In the work we report here, we typically operate at an $f \cdot d$ product less than 1 MHz-mm; for that reason, we omit from Figure 1 all higher modes such as the A1 mode which cuts off below 1.69 MHz-mm, the S1 mode which cuts off below 2.94 MHz-mm, and so on. At an $f \cdot d$ product of typical interest in our work, such as 0.5 or 0.6 MHz-mm, the S0 wave is largely non-dispersive with a group velocity that is almost constant, whereas the A0 wave is highly dispersive.

* Contact author: ijo@cmu.edu; 412-268-2950; Carnegie Mellon University, Department of Civil and Environmental Engineering, Pittsburgh, PA, 15213.

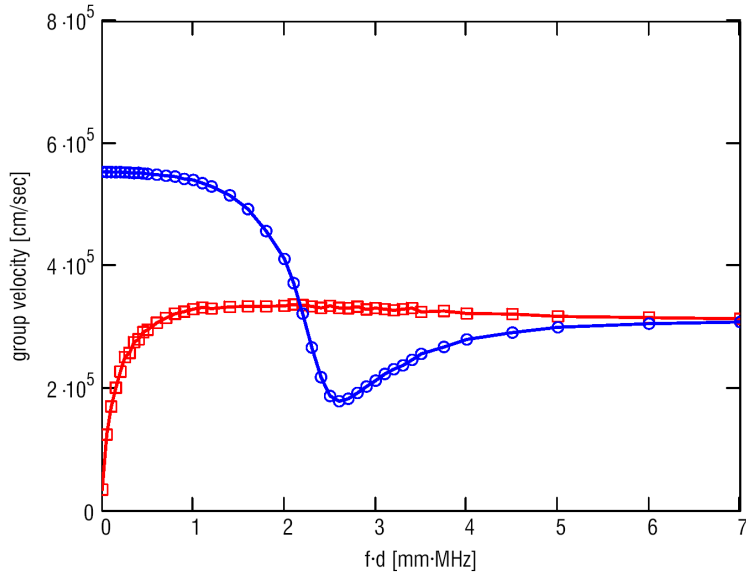


Figure 1. Dispersion curve, S0 and A0 modes ($c_L = 5.88 \text{ mm}/\mu\text{s}$, $c_T = 3.39 \text{ mm}/\mu\text{s}$.)

A solution to the complexity presented by Lamb waves, ideally, would be a transducer selectively exciting a single mode. Approaches for selective excitation include wedge (angle beam) transducers [3], comb-type transducers [4], and linear arrays with time-delayed excitation [5]. The recent use of single PZT wafers as transducers, surface-mounted to the plate, has justifiably attracted great interest [6, 7]. The inherent simplicity of wafer-type transducers is encouraging for reasons of practicality and low cost. A theoretical explanation for mode selectivity of a PZT wafer transducer, with accompanying experiments, has been published by Giurgiutiu [8], and our work was inspired in large part by those important results. We combine finite element simulation and experimental studies to explore further the operation of the wafer transducer. Our work includes a more-detailed finite element simulation of PZT wafer performance as an emitter, of resulting mode selectivity, and of PZT wafer performance as a detector; we separately model the emission and detection processes. In particular, we calculate the wave velocities and the received voltage signals due to A0 and S0 modes at an output transducer as a function of pulse center frequency. These calculations include the effects of finite pulse width, pulse dispersion, and the detailed interaction between the PZT element and the transmitting medium.

2. LAMB WAVE EXCITATION, EXPERIMENTAL RESULTS

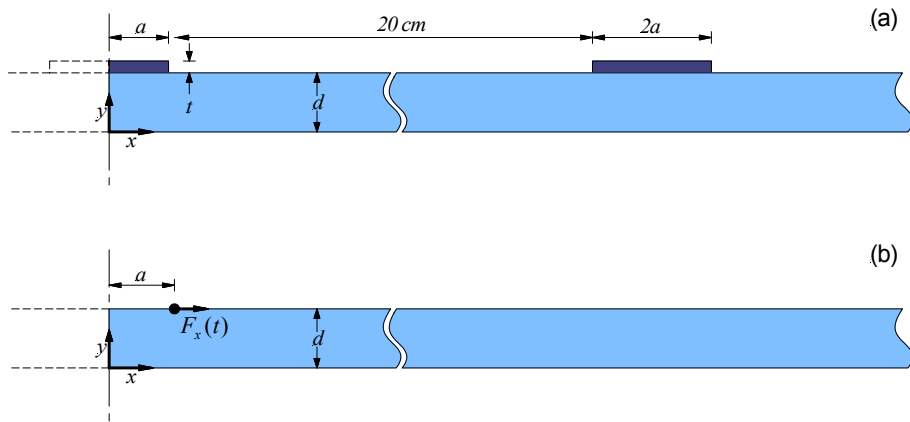


Figure 2. Geometry, plane strain, for PZT wafer experiments and simulations; symmetrical about y-axis.

Figures 2a and 2b show the plane strain geometry treated in this work. Figure 2a shows two wafer-type transducers used in our experiments; each transducer is $0.64 \text{ mm} \times 6.4 \text{ mm} \times 19.2 \text{ mm}$ ($t \times 2a \times \text{depth into page}$) and is bonded to an aluminum plate at a separation distance of 200 mm. The plate thickness d is 1.59 mm, and the transducers are surface mounted to the plate using Epotek E4110-LV silver epoxy. The transducer material is Motorola 3203HD PZT, with the poling direction normal to the plate surface. In the simulation studies, symmetry is assumed about the y-axis shown, bisecting the PZT wafer that is designated as the emitter. Figure 2b shows the simplest simulation model, in which the principal effect of the PZT wafer is represented as a point force acting in the x-direction at position $x = a$.

In our simulation and experimental studies, the emitting transducer was driven by a windowed sinusoid of the form

$$V(t) = \begin{cases} V_0 \sin(\omega t) \cdot \left(\sin\left(\frac{\omega t}{10}\right) \right)^2 & t < \frac{10\pi}{\omega} \\ 0 & \textit{otherwise} \end{cases}$$

which corresponds to the waveform shown in Figure 3.

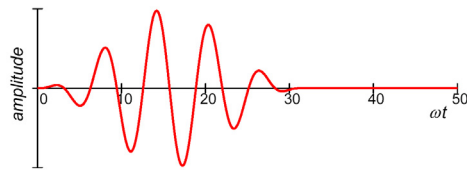


Figure 3. Exciting waveform

In our simulation and experimental studies, V_0 was 10 volts and the center frequency, f , was varied from 33 to 800 kHz. The exciting waveform was generated by a National Instruments PCI-5411 and the received pulse was recorded using a National Instruments PCI-5112 100 MHz A/D board. Typically, between 5000 and 10000 samples were acquired under computer control using Labview.

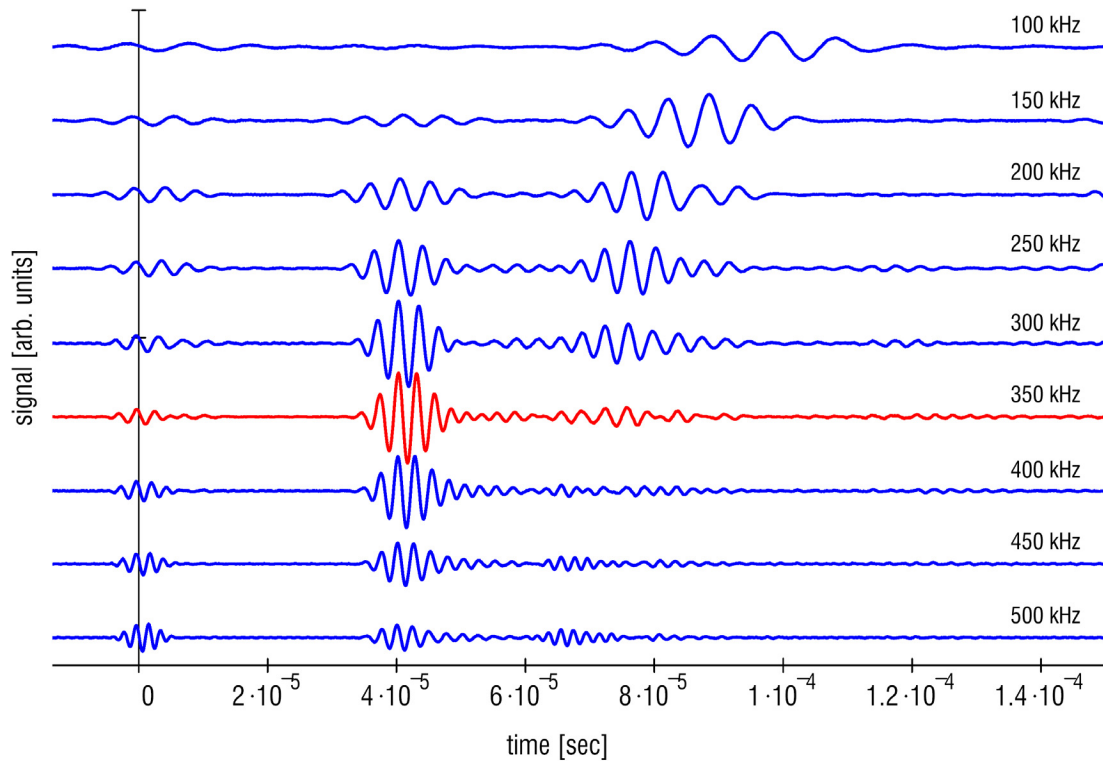


Figure 4. Received signals (experimental, 200 mm separation) as a function of frequency.

Figure 4 shows pulse transients received in experimental studies at center frequencies between 100 and 500 kHz, corresponding to $f \cdot d$ products between 0.16 and 0.8 MHz-mm. Within each transient record, two distinct arrivals are visible. The first arrival is due to the emitted S0 mode and the second to the A0 mode. The S0 mode arrives at a time that is almost independent of frequency, corresponding to the relatively nondispersive behavior of the S0 mode in the range of interest, with a group velocity of approximately 5.6 mm/ μ s. The A0 mode travels more slowly and shows significant dispersion, exhibiting a frequency-dependent group velocity ranging from approximately 2.3 to 3.5 mm/ μ s over the range of interest. This behavior is consistent with the calculated dispersion curves for aluminum.

Also apparent in these data is a strong dependence of pulse amplitude on frequency. The S0 mode arrival displays a maximum near 350 kHz, at which frequency the A0 mode has low (but nonzero) amplitude. The A0 mode arrival displays a maximum near 150 kHz, and a minimum near 400 kHz. This is the mode selectivity result for a wafer-type transducer, introduced by Giurgiutiu [8].

3. DISCUSSION OF EARLIER WORK

Giurgiutiu [8] developed an analytical solution from which he developed the basic results of mode selectivity. That analytical model had the following assumptions:

- The excitation was a point force, as shown in Figure 2b, which is only a rough approximation to the forces exerted by the piezoelectric material.
- The excitation was a steady state sinusoid, and not a pulse excitation.
- The analytical solution described the amplitude of particle displacement, or particle velocity, at any position. However, in the practical case, the output signal would be the voltage developed at a PZT wafer functioning as a detector.

Giurgiutiu's point-force, steady-state solution [8] predicted that a transducer of width $2a$ would generate maximum and minimum response, for Lamb wave mode i , at particular frequencies. The frequencies correspond to the cases where the transducer width, $2a$, equals an odd number of half-wavelengths or even number of half-wavelengths, respectively, where the wavelength is calculated from the phase velocity. The frequencies are expressed as

$$f_{\min}^{i,n} = \frac{v_{\text{phase}} \cdot (n)}{2a} \quad \text{and} \quad f_{\max}^{i,n} = \frac{v_{\text{phase}} \cdot (n - 1/2)}{2a}$$

Giurgiutiu referred to a "sweet spot" at which the S0 mode is near its maximum amplitude while the A0 mode is relatively small in amplitude; our experimental results in Figure 4 show the 350 kHz frequency to be a "sweet spot" for the transducer (width of 6.4 mm) used in our study. The mechanical properties and plate thickness enter by the dispersion curve (not shown) for phase velocity of the plate modes. For an aluminum plate with a thickness of 1.59 mm, and a transducer with a width of 6.4 mm, the equations above predict a peak in the S0 mode at 419 kHz, a null in the S0 mode at 816 kHz, a peak in the A0 mode 86 kHz, and a null in the A0 mode at 283 kHz.

4. SIMULATION OF TRANSDUCER EMISSION PERFORMANCE

We simulate the transient generation of plate waves in an infinitely wide plate using plane-strain finite element analysis, simulating a two-dimensional wave generated by the transient excitation pictured in Figure 3. We first simulate the effect of a point force in the longitudinal direction, as employed in the Giurgiutiu [8] analytical model, and we then simulate the interaction between a PZT wafer and the plate, which more accurately matches the actual physical configuration. Full details of our simulation studies are reported elsewhere [9]; in this paper we describe our simulation results, we compare them to Giurgiutiu's analytical results, and we compare them to our experimental measurements.

Referring to Figure 2b, we apply a point force to the upper surface at position $x = a$. Displacement x is constrained to be zero at $x = 0$, and consequently we model one half of a symmetric domain while all other boundaries are free. Simulations were performed in the time dependent mode with output time steps typically equal to one eighth of a period. Mesh parameters were chosen so that the element sizes were substantially smaller than a wavelength. Simulations were repeated with a halved time step, and with smaller element size, to verify model convergence. Emission simulations were performed using the time-stepping mode of the two-dimensional plane strain mode of FEMLAB 2.3 (ode23s solver). In all simulations reported below, the plate was aluminum ($E = 70$ GPa, $\rho = 2700$ kg/m³, $\nu = 0.33$, mass damping coefficient = 0, stiffness damping coefficient = 0) with a thickness of 1.59 mm, and the force was applied at $x = 3.2$ mm. These dimensions were chosen to match the configuration used in all experiments.

Figure 5 shows simulation results, for excitation frequencies between 100 and 500 kHz, at $t = 40$ μ s. The wave is generated at the left and propagates to the right, and the plate thickness is exaggerated by a factor of two. Color contours indicate the von Mises stress, and arrows indicate the vector particle displacements from the equilibrium position. We see two propagating modes with clearly different character. The S0 mode has the highest group velocity and shows particle displacements mostly in the x direction along the direction of propagation. There is a small dilation and expansion in the y direction, which is symmetric about the center of the plate, due to the Poisson effect. The slower wave is the A0 mode, which shows particle displacements that are mostly in the y direction and are asymmetric about the center of the plate. The propagation velocity of the A0 mode is smaller than that of the S0 mode, and increases with frequency. Qualitatively, it appears that the relative magnitudes of the A0 and S0 modes vary, with a minimum magnitude for the A0 mode near 300 kHz. This agrees well with the frequency where the wavelength of the A0 mode is equal to the total length of the force baseline. The propagation velocity of the A0 mode increases with frequency and the emitted intensity reaches a minimum near 300 kHz.

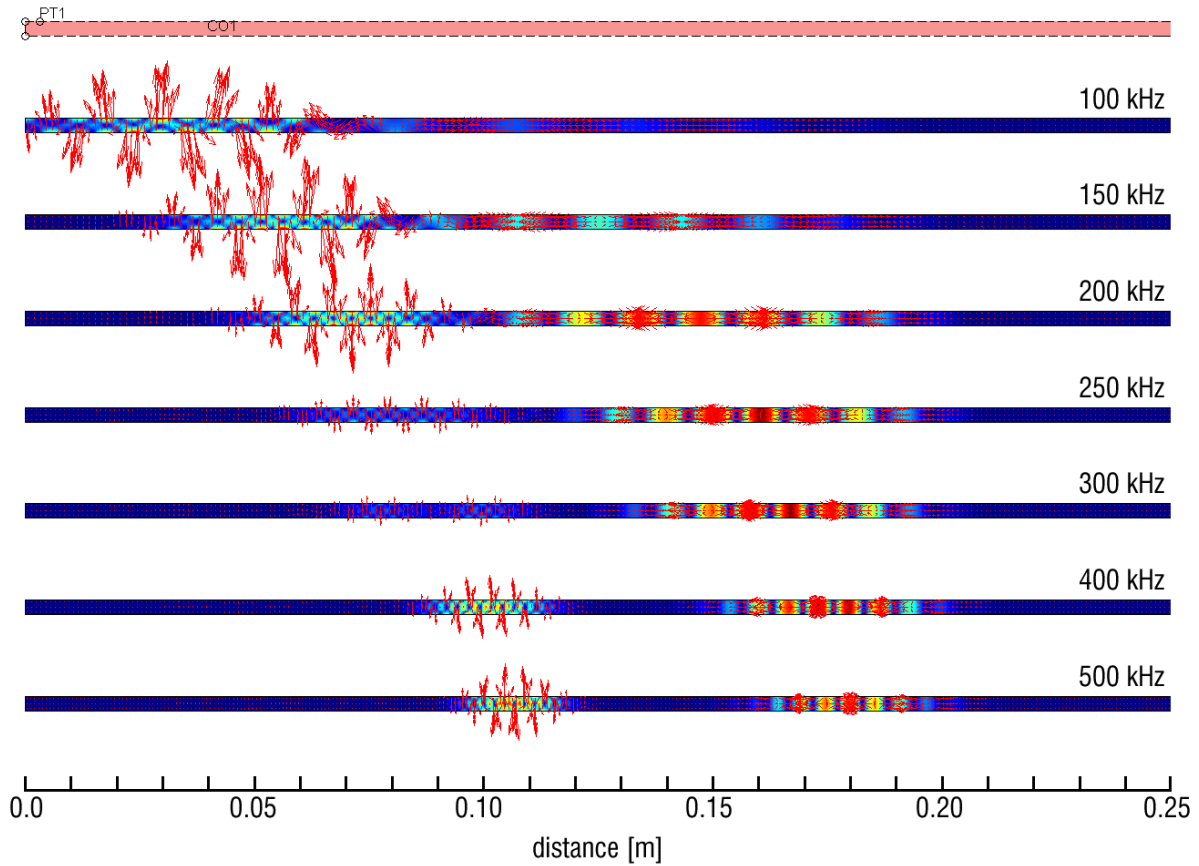


Figure 5. Emission of A0 and S0 waves by a point-force source, $t = 40 \mu\text{s}$

The point-force excitation represents a highly idealized model, and therefore we performed finite element simulations of a PZT emitting element bonded to the aluminum plate, as pictured in Figure 2, with details described elsewhere [9]. We employed both a full “multiphysics” electromechanical model of the piezoelectric material, as well as a simpler approach that we termed a “PZT-force” model. In the PZT-force model, we represented the transducer, for purposes of emission, by an appropriate set of forces in the x and y directions. The PZT-force model was more efficient computationally, and comparisons showed that it produced simulation results essentially identical to those produced by the full multiphysics model.

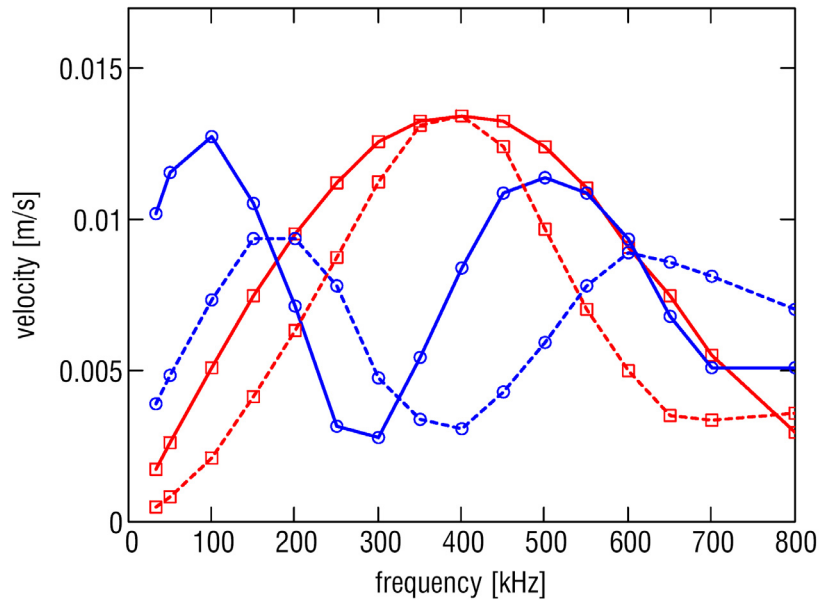


Figure 6. Maximum particle velocity, at 10 V excitation

Figure 6 summarizes the emission simulation results by plotting maximum particle velocity, observed at a point 200 mm distant from the origin, against excitation frequency. The curves in red, with the single peak near 400 kHz, correspond to the S0 mode, and the curves in blue, with two peaks, correspond to the A0 mode. The solid lines are results using the point-force model, and the dashed lines are results using the PZT-force model; the amplitude for the point-force model was scaled to match the PZT-force model at the peak of the S0 mode.

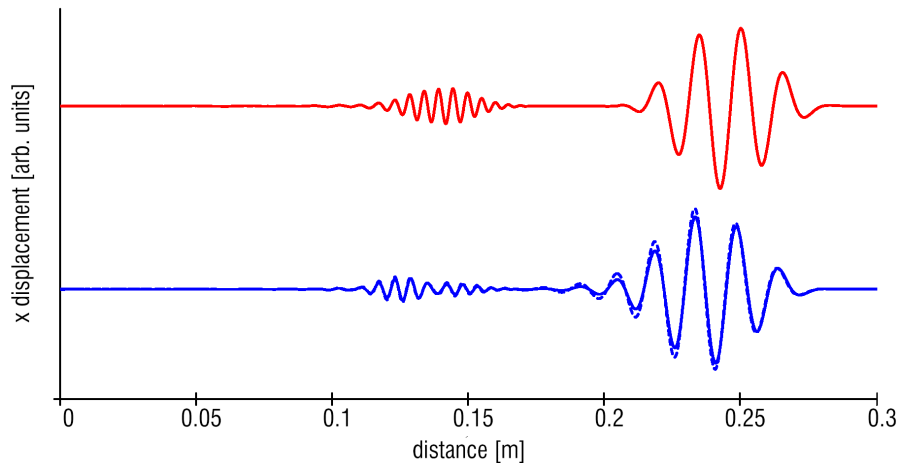


Figure 7. Surface displacement in x-direction, $t = 53 \mu\text{s}$

To further confirm that the PZT-force model is a good approximation, we performed full multiphysics simulations at selected frequencies. Figure 7 compares results from the full multiphysics model with those from the point force model and the PZT-force model. It plots the surface x-displacement at an arbitrary point in time, $53 \mu\text{s}$, for an excitation at 350 kHz. The top plot is obtained using the point-force model, scaled to match the peak amplitude of the multiphysics mode. The bottom plot contains two records, one (solid line) obtained using the PZT-force model and another (dashed line) obtained using the full multiphysics model. Agreement between the PZT-force model and the full multiphysics model is excellent, both in the magnitude and detailed shape of the waves. As might be expected, there are differences between the point force model and the other two models, even when point force results are scaled to fit the S0 wave amplitude.

5. SIMULATION OF TRANSDUCER DETECTION PERFORMANCE

We next consider Lamb wave detection. Because detection is the inverse of emission, it may appear at first glance that wave detection curves, as functions of wave mode and frequency, should be the same as the curves in Figure 6. However, this is most definitely not the case, for a number of reasons. For example, the assumption of symmetry applicable to the emission model has no counterpart in the detection model. Similarly, in contrast to the physical principles of wave emission, during detection a decrease in signal is not expected at frequencies where the size of the element is shorter than a half wavelength. At these frequencies the detection is expected to show constant sensitivity, since there is no partial cancellation as is the case in the wave generation.

Simulating Lamb wave detection required a full multiphysics (coupled electro-mechanical) model. The simulations were performed using the multiphysics (electrostatics plus plane-strain structural mechanics) time-dependent mode of FEMLAB 3.0: the direct (UMFPACK) linear solver in the weak mode. The response of a receiving PZT 6.4 mm long and 0.64 mm thick was calculated separately for S0 and A0 modes. A particular wave mode was selectively generated by two point forces on the top and bottom of the aluminum plate, driven in phase to launch the S0 mode and driven out of phase to launch the A0 mode. The bottom surface of the PZT detector was electrically grounded and an equipotential boundary condition was set on the top surface. The simulation yields the time-dependent mechanical displacements and also the time-dependent potential of the PZT top surface. The sensitivity for each mode was calculated by dividing the maximum top surface potential by the particle velocity for each wave.

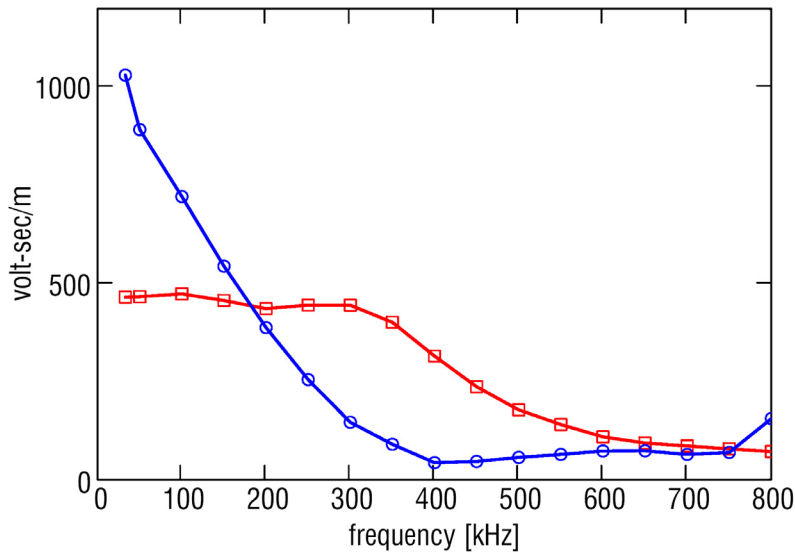


Figure 8. PZT wafer detector voltage, at particle velocity of 1 m/s

Figure 8 summarizes the detection simulation results, plotting detector voltage against excitation frequency, for a peak particle velocity of 1 m/s. The red curve (squares) corresponds to the S0 mode, and the blue curve (circles) corresponds to the A0 mode. Considering first the sensitivity to the S0 mode, at low frequencies the sensitivity of the PZT wafer is practically constant. In this frequency range, the half-wavelength of the acoustic wave is longer than the PZT wafer, and therefore the wafer functions as an ideal strain sensor. At higher frequencies the PZT is more than a wavelength long, and the strain reverses sign along the transducer, leading to a decrease in sensitivity.

Transducer sensitivity to the A0 mode is different, because strain is related to particle velocity through the expression

$$S = \frac{du}{dx} = \frac{du}{dt} \frac{dt}{dx} = \frac{du}{dt} \frac{1}{c_p}$$

where S is the strain, u is the particle displacement, and c_p is phase velocity.

The phase velocity of the A0 mode is strongly frequency-dependent and decreases toward zero at low frequencies. Therefore, the A0 sensitivity increases strongly with decreasing frequency, as shown in Figure 8. Additionally, we see evidence for the expected minimum near 400 kHz, where the transducer is exactly one wavelength long, and a maximum near 600 kHz, where it is exactly 1.5 wavelengths long.

6. CALCULATION OF SYSTEM TRANSFER FUNCTION

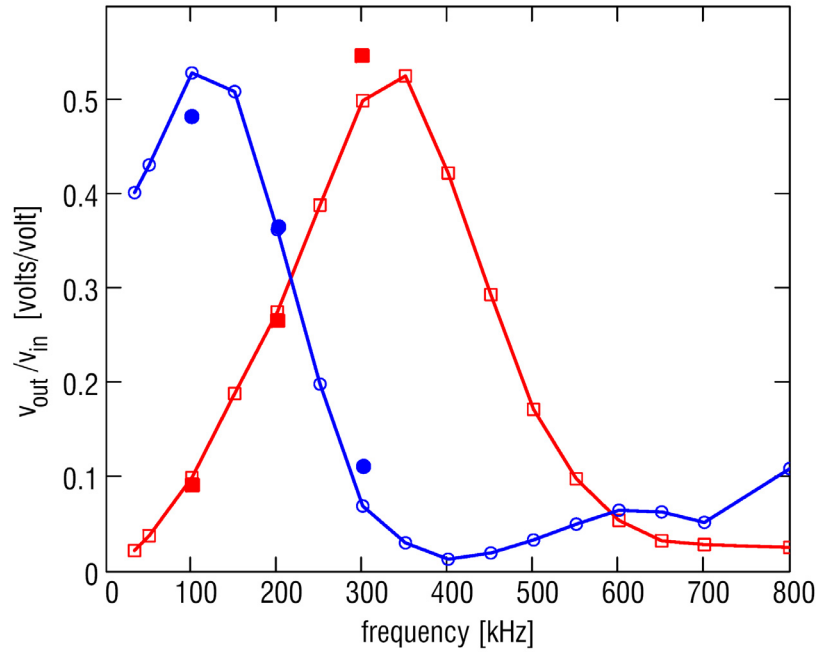


Figure 9. Overall system transfer function, v_{out}/v_{in} , as a function of pulse center frequency

To predict the detected signal, in volts, for a given excitation amplitude, in volts, we multiply the particle velocity per volt, from Figure 6, by the detection sensitivity, in volts per unit particle velocity, from Figure 8. This is the overall system transfer function v_{out}/v_{in} and is shown in Figure 9 as a function of the pulse center frequency. Again, the red curve (squares) corresponds to the S0 mode and the blue curve (circles) corresponds to the A0 mode. The S0 and A0 peak locations are near to the predictions, with the S0 peak lower in frequency and the A0 peak somewhat higher. For this geometry, generation of the S0 mode is predicted to be strongly dominant near 325 kHz. In Figure 9 we also show results for v_{out}/v_{in} obtained from a full end-to-end multiphysics calculation, plotted as solid (red) squares for the S0 mode and solid (blue) circles for the A0 mode. These calculations are highly time-consuming, particularly at the extremes of high and low frequencies and therefore we performed them only at a few selected frequencies. The results shown in Figure 9 are in very good agreement with those obtained by separate simulation of the emission curve and the detection sensitivity curve. This observation further supports the accuracy of the PZT force model for more efficient simulation of wave emission.

6. COMPARISON WITH EXPERIMENTAL RESULTS

We performed an extensive series of experiments for comparison with the simulated transfer function shown in Figure 9. We used an aluminum plate with a thickness of 1.59 mm, with two PZT transducers (Motorola 3203HD) each 6.4 mm × 19.2 mm × 0.64 mm. The transducers were mounted using silver epoxy (Epotek E4110-LV) with their long sides parallel, spaced approximately 200 mm apart. The transducers were far from the edges of the aluminum plate, so that pulses from edge reflections were delayed by sufficiently to avoid interference with the first received A0 pulse. The

emitting transducer was excited through a National Instruments PCI-5411 board, programmed to produce the windowed sinusoidal pulse with peak amplitude of 10 V. The detector was read by a National Instruments PCI-5112 analog input board with a bandwidth of 100 MHz; between 5000 and 10000 samples were typically collected for each record.

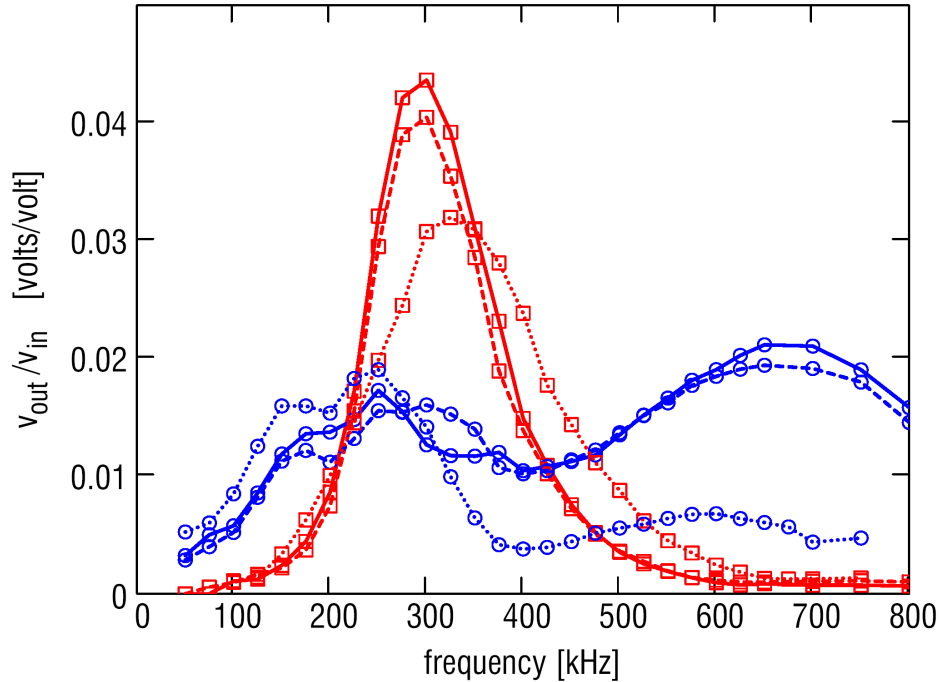


Figure 10. Measurements of v_{out}/v_{in} , repeated for three transducer pairs

Figure 10 shows v_{out}/v_{in} plotted as a function of frequency, for three different transducer pairs. The red curves (squares) correspond to the S0 mode arrival and the blue curves (circles) correspond to the A0 mode arrival. The results obtained for different transducer pairs are quite similar for the S0 mode in both amplitude and frequency dependence, while the A0 results are significantly different. For the S0 mode, we observe good agreement between experiment and theory with respect to the peak position and the frequency dependence. For the S0 mode, the peak experimental response occurs near 300 or 325 kHz, compared to the simulated peak near 350 or 400 kHz shown in Figure 9. The agreement between experiment and simulations for the A0 mode is poor, with the simulations predicting a peak amplitude much higher than observed, and predicting the peak to occur at a substantially lower frequency than observed.

We have ruled out instrumental artifacts as an explanation for the discrepancy between simulations and experiment. We attribute the poor agreement between the A0 experiment and simulation to imperfect bonding between the PZT wafer and the aluminum sheet. This is supported by our observations of differences in the measured impedance spectrum for different transducers which are consistent with imperfect bonding (not shown). Apparently the A0 mode is more sensitive to the bonding conditions than the S0 mode. It is important to note that the published measurements by Giurgiutiu [8] show that with appropriate bonding conditions results in better agreement with simulations can be obtained. We also note that the S0 mode may be preferable in applications because it can be generated selectively and because it exhibits little dispersion over a wide frequency range.

7. PULSE-ECHO DAMAGE DETECTION

Pulse-echo flaw detection experiments were performed on the setup described previously in section 2. One transducer, located 310 mm from the nearest panel boundary, was driven at 6.5 V (peak-to-peak) with a pulse center frequency of 350 kHz. Reflections from distant boundaries returned with ample signal strength (tens of mV) after a travel distance in

excess of 2 m. A part-thickness flaw, 80 mm long, was cut into the plate parallel to the boundary, 240 mm from the transducer and 70 mm from the boundary. Signals were recorded, with 100X averaging, before the flaw was introduced and then as the flaw depth reached approximately 0.2, 0.6, and 0.9 mm.

Figure 11 shows the four signals, offset from each other along the y-axis and arrayed top to bottom, through $t = 200 \mu s$. The prominent arrival in each signal near $130 \mu s$ is the S0 reflection from the boundary, over a path length of 620 mm. The S0 reflection from the flaw is expected to arrive near $100 \mu s$, and is visible in the bottom two records.

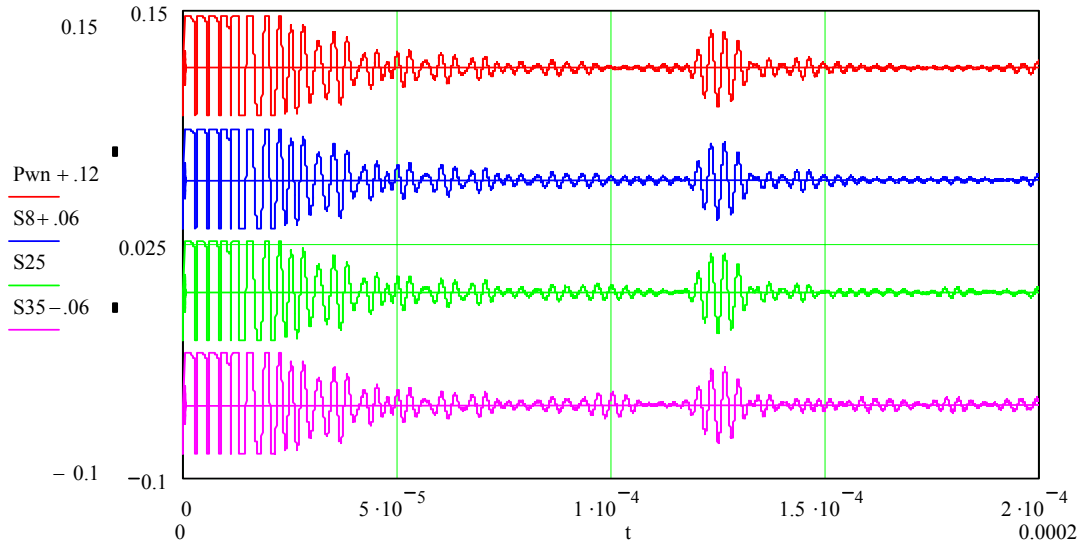


Figure 11. Signals received at transducer at flaw depth of 0.0, 0.2, 0.6, and 0.9 mm

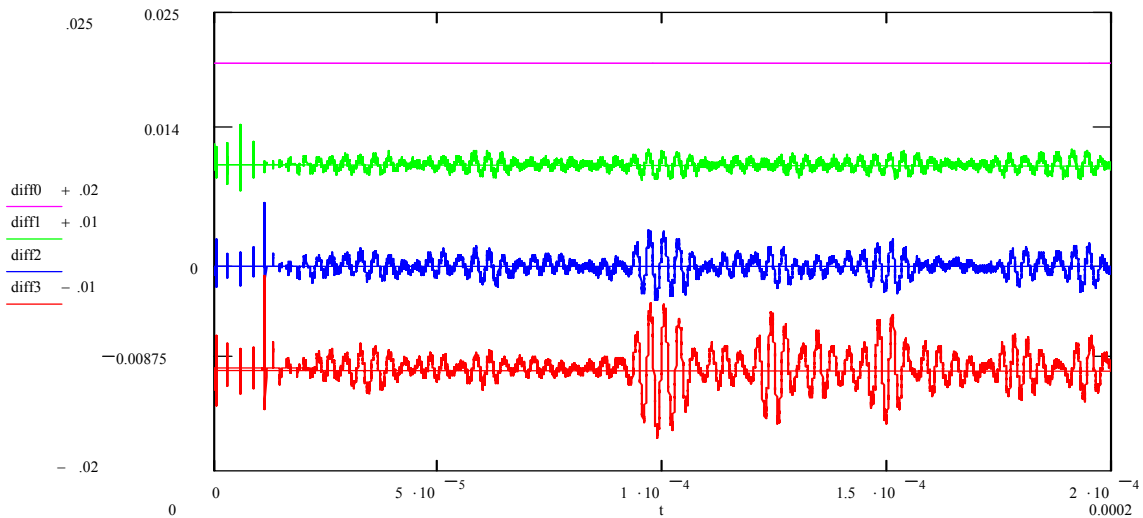


Figure 12. Difference with respect to unflawed signature

Figure 12 shows the differences with respect to the signal for the unflawed case. We observe that the S0 reflection from the flaw, at approximately $100 \mu s$, is easily detected.

8. CONCLUSIONS

In this paper, the operation of a PZT wafer transducer was analyzed for the emission and detection of Lamb waves using a combination of finite element simulation and experiments. Experimental studies demonstrated the characteristic properties of the S0 and A0 wave modes generated by an appropriate transient excitation, for values of the f-d product between 0.16 and 0.80 MHz-mm. Finite element simulations accounted for the detailed mechanical interactions between the transducer and the transmitting medium. A point-force model was shown to be a useful tool to analyze the qualitative behavior of the transducer. Two more-advanced models were then introduced: a PZT-force model, and a full multiphysics model. For wave emission the PZT force model and the full multiphysics model were closely comparable, but for wave detection the full multiphysics model was necessarily used. The simulations and the experimental results showed that a piezoelectric wafer transducer can be used for selective excitation of the S0 mode. The overall system transfer function was obtained from the simulation results, and showed reasonable agreement with experimental results for behavior of the S0 mode, and poor agreement with experimental results for behavior of the A0 mode.

Initial experimental results were presented for one example of pulse-echo flaw detection. A single PZT wafer-type transducer, excited at 6.5 V, produced reflected signals of ample strength (tens of mV) from distant boundaries in an aluminum plate. Reflections from a part-thickness flaw were detected at a flaw depth of roughly 0.6 mm, less than 40% of the plate thickness.

ACKNOWLEDGEMENTS

The authors wish to acknowledge support from the Bosch Research and Technology Center North America, Pittsburgh, Pennsylvania, and from the National Science Foundation under grant CMS-0329880. Any opinions, findings, and conclusions or recommendations expressed in this material are those of the authors and do not necessarily reflect the views of the National Science Foundation.

REFERENCES

1. Rose, J. L., *Ultrasonic Waves in Solid Media*, Cambridge University Press, 1999.
2. Graff, K. F., *Wave Motion in Elastic Solids*, Oxford University Press, 1975.
3. Rose, J. L., "Guided wave nuances for ultrasonic nondestructive evaluation," *IEEE Trans. Ultrasonics, Ferroelectrics, and Frequency Control*, Vol. 47, 575-583, 2000.
4. Rose, J. L., Pelts, S., and Quarry, M., "A comb transducer model for guided wave NDE," *Ultrasonics*, Vol. 36, 163-168, 1998.
5. Li, J., and Rose, J. L., "Implementing guided wave mode control by use of a phased transducer array," *IEEE Trans. Ultrasonics, Ferroelectrics, and Frequency Control*, Vol. 48, 761-768, 2001.
6. Kessler, S.S., Spearing S.M. and Soutis, C., "Structural health monitoring of built-up composite structures using Lamb wave methods," submitted to *Journal of Intelligent Material Systems and Structures*, 2003.
7. Giurgiutiu, V., and Zagrai, A.N., "Characterization of piezoelectric wafer active sensors," *Journal of Intelligent Material Systems and Structures*, Vol. 11, 959-975, 2000.
8. Giurgiutiu, V., "Lamb Wave Generation with Piezoelectric Wafer Active Sensors for Structural Health Monitoring," SPIE Smart Structures Conference, San Diego, 2003.
9. Nieuwenhuis, J. H., Neumann, J., Greve, D. W., and Oppenheim, I. J., "Generation and detection of guided waves using PZT wafer transducers," submitted to *IEEE Trans. Ultrasonics, Ferroelectrics, and Frequency Control*, 2004.